09

Photonic integrated circuit for a wavelength stabilization system of a tunable C-band laser

© A.A. Sheynberger, V.E. Trutneva, M.V. Stepanenko, Yu.S. Zhidik, I.V. Yunusov

Tomsk State University of Control Systems and Radioelectronics, Tomsk, Russia
E-mail: annasejnberger@gmail.com

Received December 8, 2025
Revised February 6, 2026
Accepted February 6, 2026

The article presents the results of developing a photonic integrated circuit (PIC) for measuring the wavelength (frequency) of radiation in the C-band. The developed PIC provides a measurement resolution of 2.4 pm (0.3 GHz), an accuracy of ±8 pm (±1 GHz), and a sensitivity to optical power of −18 dBm. The PIC was developed for manufacturing using SOI technology. This PIC can be used as a part of a system for stabilizing the wavelength of radiation from a tunable C-band laser when implementing DWDM technology.

Keywords: measurement of radiation wavelength, stabilization of radiation wavelength, DWDM, tunable laser.

DOI: 10.61011/TPL.2026.05.63298.20591

A tunable laser is an integral part of fiber optic communication lines (FOCL), which use dense wavelength division multiplexing (DWDM) technology. To ensure the compatibility of the equipment from different manufacturers and to create the scalable networks, the frequency grid in the DWDM technology is governed by international standard ITU-T G.694.1, which is developed by the International Telecommunications Union-Telecommunications Standardization Sector. Deviations of the laser emission wavelength from the standardized values cause bit errors in transmission of information along FOCL [1,2]. This makes the laser emission wavelength stabilization systems, which include photonic integrated circuits (PIC) for wavelength measurement, popular. When the DWDM technology is implemented according to ITU-T G.694.1 standard with the frequency grid of 12.5 GHz such PIC must provide for the accuracy of wavelength (frequency) measurement not below ±0.05 nm (±6 GHz).

To measure the wavelength of emission, demultiplexers may be used in PICs [3]. The integral demultiplexers are based on arrayed waveguide gratings (AWG) or planar concave gratings. PICs with demultiplexers provide for high-speed measurements with resolution of up to 1.2 nm [4]. The significant disadvantage of such solutions is the large area of diffraction waveguide gratings and inability to manufacture planar concave gratings on standard silicon-on-insulator (SOI) substrates with the thickness of the working layer of 220 nm. This type of substrates contains a silicon dioxide layer placed between the layers of single crystal silicon. Besides, the SOI platform is preferable for PIC due to high optical contrast, ability to use the plates of up to 300 mm and compatibility with SOI CMOS-technology, which provides for low cost, large-scale manufacture and integration of photon and electron circuits on a single plate or chip [5,6].

Another approach to measurement of emission wavelength includes microring resonators (MRR). For example, paper [7] presents a PIC with four MRRs providing for resolution of the wavelength measurement of up to 1.6 pm and precision of 15 pm. However, this solution is developed for implementation on the basis of the technological InP platform, whereas a SOI technological platform is believed to be more promising.

This paper is dedicated to the development of PIC for measurement of tunable laser wavelength in C-band (1530−1565 nm), which may be manufactured using the technology compatible with SOI CMOS technology.

The proposed PIC consists of an MMI-splitter 1×4 (MMI — multimode interference), four MRRs with different lengths of circumference of a ring waveguide (MRR1−MRR4 in Fig. 1), four thermooptical phase shifters (PHS1−PHS4 in Fig. 1) and four photodiodes (PD1−PD4 in Fig. 1), each of which is connected to MRR.

Emission via an MMI-splitter 1×4 is sent to four MRRs. Control voltage at each phase shifter (PHS) varies from achievement of resonance (maximum signal attenuation) in the corresponding MRR, which results in reduction of current at the output of the corresponding photodiode (PD). Therefore, each value of resonant wavelength of emission corresponds to the set of the values of control voltage on PHS, at which the minimum current is observed on all four PDs. Resolution of the wavelength measurement for this PIC is determined by the step of MRR resonant peak position at minimum change of the control voltage. Precision of measurement in its turn is determined by the width of the resonant peak at half maximum designated as FWHM (full width at half maximum). Development of PIC proposals reduces to the development of MMI-splitter 1×4 and four MMRs, and also to the theoretical study of PIC.

The MMI-splitter 1×4 must provided for the minimum introduced optical losses and split the optical power evenly

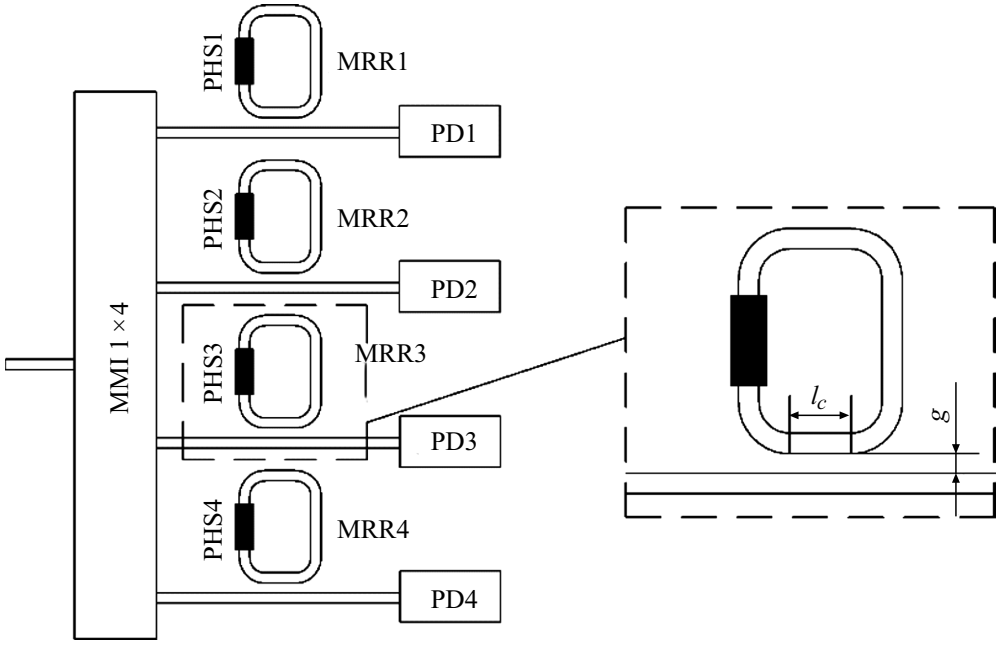

Figure 1. Schematic image of PIC for measurement of emission wavelength.

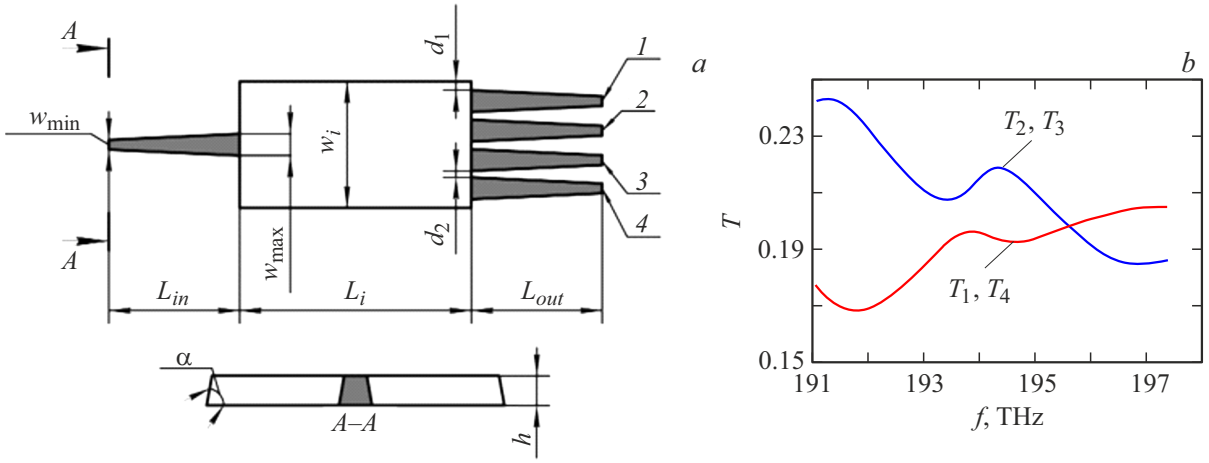

Figure 2. Geometric parameters (a) and spectral dependences of coupling efficiencies (b) of the developed MMI-splitter 1 × 4 (T_1–T_4 — coupling efficiencies for outputs 1–4 respectively).

in the operating wavelength (frequency) range. For this purpose it is necessary to optimize its geometric parameters (Fig. 2, a). Besides, some parameters of the device are regulated by the technology of its manufacture, namely $h = 0.22\,\mu$m, $\alpha = 85°$, $w_{min} = 0.45\,\mu$m. Similar technologies are described in papers [8,9]. Refractive indices of Si and SiO_2 at the central frequency are equal to 3.467 and 1.449 accordingly. The distance d_2 must be at least $0.8\,\mu$m to minimize crosstalk (when this condition is met, the coupling efficiency between the adjacent waveguides has the maximum permissible value 10^{-4}). The tapered shape of waveguides is required to match the fields of modes in a single-mode waveguide and interference area, where several modes propagate.

Width w_i was specified as equal to $5\,\mu$m, to locate four output waveguides at the output of the MMI-splitter whilst complying with the requirement to the distance between them. Width w_{max} was specified as equal to $0.5\,\mu$m, which is also specified by the requirements to the distance between the waveguides. The input waveguide was located in the middle of the interference area width. The positions of the output waveguides were determined by distribution of the electric field in the interference area calculated using EME (eigenmode expansion) method [10]. The optimal values of other geometric parameters were determined by their variation. Upon variation of every parameter the other parameters had fixed values. Absorption of optical power by silicon and its scattering on irregularities of the walls

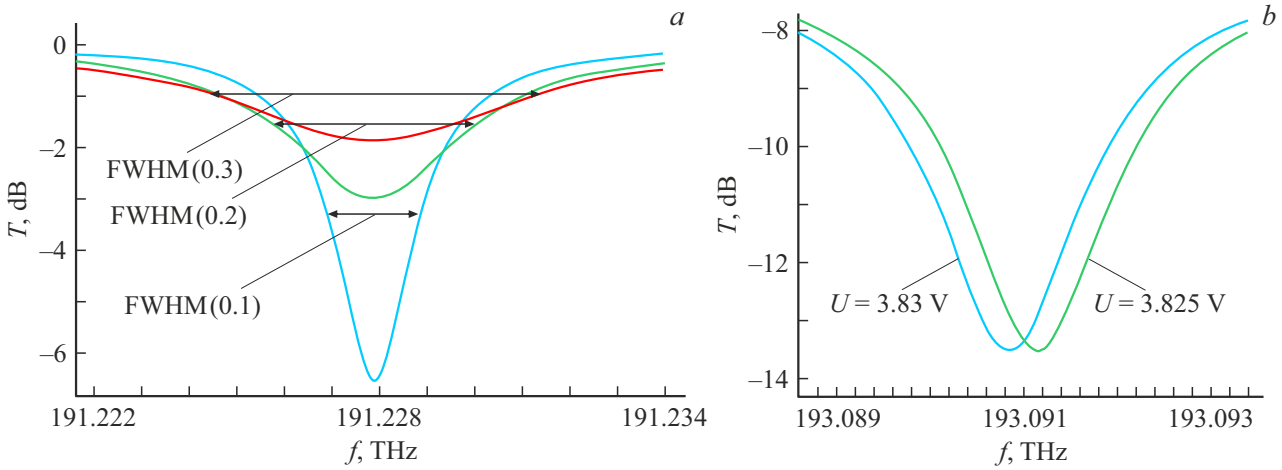

Figure 3. Results of calculations using the compact model method. *a* — influence of MRR coupling coefficient at its resonance spectrum at the absence of control voltage on PHS; *b* — displacement of the resonance peak of MRR at minimum available change of control voltage at PHS.

in modeling were not taken into account. As a result, the following optimal values of MMI-splitter geometric parameters were identified: $w_i = 5\,\mu$m, $w_{\max} = 0.5\,\mu$m, $L_{in} = 12\,\mu$m, $L_{out} = 10\,\mu$m, $L_i = 10.6\,\mu$m, $d_1 = 0.25\,\mu$m, $d_2 = 0.8\,\mu$m.

Fig. 2, *b* presents the estimated spectral dependences of transmission coefficients for the designed MMI-splitter 1×4. Transmission coefficients are numbered in accordance with the numbers of output waveguides in Fig. 2, *a*. Since the steps between the standard DWDM channels are multiple to 12.5 GHz, in the calculations and presentation of their results it is feasible to change from wavelength in nm to frequency (f) in THz.

Therefore, the developed MMI-splitter is characterized by rather weak spectral dependence of coupling efficiencies in the operating band.

MRR development reduces to the determination of those values of the circumference length of the ring waveguide and the coefficient of its coupling to the direct waveguide, which provide for the highest precision and resolution of the emission wavelength measurement. The compact model method [6] was used to study the effect of the coupling coefficient of MRR at its resonance spectrum and FWHM in the absence of the control voltage at PHS. The length of circumference of the ring waveguide was selected as equal to 551 μm. This is the minimum value making it possible to locate a thermooptical PHS based on TiN film on the ring waveguide to modify the signal phase by 2π with control voltage supply of not more than 5 V. The PHS length was determined using the following formula:

$$l_{\text{PHS}} = (2U_{2\pi}^2 w)/(P_{2\pi}\rho_{\square}),$$

where $U_{2\pi}$ — target control voltage to change the phase by 2π, accepted as equal to 5 V in this case; w — width of TiN film equal to 1.5 μm; $P_{2\pi}$ — target electrical power necessary to rotate the phase of the phase shifter by 2π (in this case 18 mW); $\rho_{\square}$ — specific surface resistivity of thin TiN film.

The length of the TiN film was 360 μm. For compactness, two identical PHSs were used, being located at long sides of the ring waveguide. At arc bend radius 10 μm, length of contact sites 10 μm, a gap between arcs and contact sites of 10.5 μm and coupling length (l_c in Fig. 1), equal to 3 μm, the minimum length of circumference of MRR ring waveguide was around 551 μm. The intrinsic Q factor for such MRR is, according to the calculations, 58,444.99.

The values of 0.1, 0.2 and 0.3 were assigned in series to the coupling coeffciient. The loaded Q factor of MRR at the same time was 55 059.82, 46 908.85 and 37 625.48 accordingly. According to the results of the calculations, at the coupling coefficient of 0.1 the least value of FWHM is achieved, equal to 2 GHz (Fig. 3, *a*). Accordingly, the precision of frequency (wavelength) measurements is ± 1 GHz (± 8 pm). This precision of measurements is sufficient to implement the DWDM technology with the minimum standard frequency grid of 12.5 GHz in accordance with ITU-T G.694.1 standard, and is also equal to the precision of measurement of the foreign analog described in [11]. Therefore, for the device implementation the coupling coefficient of 0.1 was selected. It is important to note that the critical coupling coefficient for MRR in this case is 0.4. However, the use of MRR with the coupling coefficient that is less than the critical one is a permissible solution for the measurement devices, where the precision of measurement is more important than the minimization of losses [12].

As a result of calculation using the FDTD (finite difference time domain) method, it was found that the coupling coefficient of 0.1 is achieved at the gap between the straight and ring waveguides $g = 0.225\,\mu$m and coupling length of $l_c = 3\,\mu$m (Fig. 1). It was decided to use such shape of ring waveguides, at which the values of g and l_c are identical for all MRRs at individual values of lengths of circumferences of ring waveguides.

Table 1. Results of calculation of MRR circumference lengths

MRR number	FSR, GHz	L, μm
1	124.9	551
2	123.7	556.5
3	113.6	606.2
4	104.1	661.3

Besides, the precision of frequency measurement was also determined at the deviation of the waveguide width by $\pm 0.03\,\mu$m and deviation of their thickness by $\pm 0.01\,\mu$m (in accordance with the data on process allowances). As a result, it was established that as the width deviates by $\pm 0.03\,\mu$m the precision of measurement deteriorates down to ± 2 GHz. Besides, the precision does not depend on the thickness of waveguides in the studied range.

The principle of action of the proposed PIC requires that all MRRs have one common resonance peak within the working principle. For this purpose each MRR must have its unique value of FSR (free spectral range), which is determined by the length of circumference of the ring waveguide.

The length of circumference of the first ring waveguide L_1 was specified as equal to the minimum permissible value ($551\,\mu$m). The length of circumference of the second ring waveguide L_2 was calculated using the following formula [7]:

$$L_2 = L_1 + c/(n_g \cdot \mathrm{FSR}_{1\text{-}2}),$$

where c — speed of light in vacuum; n_g — group refractive index of the waveguide equal to 4.358; $\mathrm{FSR}_{1\text{-}2}$ — total free spectral range of the first and second MRRs.

The value $\mathrm{FSR}_{1\text{-}2}$ must be equal to the working range of the device or exceed it. In this paper the value 12.4 THz (100 nm) was selected. FSR for MRR3 and MRR4 must meet the following conditions:

1) $\mathrm{FWHM} \leqslant \mathrm{FSR}_1 - \mathrm{FSR}_3 \leqslant 12.5$ GHz;
2) $\mathrm{FWHM} \leqslant \mathrm{FSR}_1 - \mathrm{FSR}_4 \leqslant 25$ GHz.

Compliance with these conditions prevents ambiguity of emission wavelength detection related to the closeness of non-matching resonance peaks of MRR1 and MRR2, and also provides for the compliance of PIC with the requirements of frequency grids of 25 and 12.5 GHz, regulated by ITU-T G.694.1 standard. The calculation results are presented in Table 1.

Further to assess the resolution of the measurement provided for by the developed PIC (Fig. 1), it was studied by the compact model method. The shifts of MRR resonant peaks were studied at minimum available change of control voltage at PHs (5 mV). For this purpose the compact model accounted for the pre-calculated dependence of the effective refractive index of the ring waveguide on the control voltage. In particular, the change in the control voltage from 3.825 to 3.83 V causes increase in the effective refractive index by $7.55 \cdot 10^{-6}$. According to the results (Fig. 3, *b*), the resolution of the emission wavelength for this PIC is 0.3 GHz. Therefore, by resolution of measurement the developed PIC is superior to the known analogs described in [11,13], for which the measurement resolution is < 1 GHz and ~ 1.4 GHz respectively (Table 2). Besides, the deviations of width and thickness of the MMI-splitter and waveguides from target values within the process allowance do not influence the measurement resolution. It is important to note that the difference between the optical losses in Fig. 3, *a* and *b* is caused by the fact that the results presented in Fig. 3, *a*, are obtained for MRR as such, and

Table 2. Comparison of developed PIC with analogs

Source	Resolution (wavelength/ frequency)	Precision of measurement	Sensitivity (optical power)	Platform (technology)	Architecture circuits
This study	2.4 pm/$\sim$ 0.3 GHz	± 8 pm (± 1 GHz)	-18 dBm (input threshold)	Silicon on insulator (SOI)	Multi-ring resonator (Vernye)
[7]	1.6 pm/$\sim$ 0.2 GHz*	Clearly not specified (target level $\sim$ 15 pm)	Not specified (InP integral photo diodes)	InP	Multi-ring resonator (with phase modulators)
[11]	$\sim 5-8$ pm/< 1 GHz	± 8 pm	Not specified (highly sensitive photo diode on crystal)	Silicon (CMOS-compatible, athermal)	Interferometers Mach–Zender (compensated by temperature)
[13]	$\sim$ 11 pm/$\sim$ 1.4 GHz	Not specified	Not specified	Si_3N_4	Ring resonant cavity + AWG (two-cascade)

*Frequency value is obtained theoretically.

Table 3. Estimated values of control detection voltage

f, GHz	U_1, V	U_2, V	U_3, V	U_4, V
195.90	2.625	1.505	2.365	2.125
193.1125	3.495	3.265	0.725	1.64
193.1	3.695	3.48	1.405	2.015
193.0875	0.895	3.68	1.845	2.36
191.60	0.375	0.65	2.31	3.11

the results presented in Fig. 3, *b*, — for the MRR included into the circuit diagram that includes an cMMI-splitter1 × 4 and four MRRs.

Table 3 presents the estimated values of control voltages at thermooptical PHSs, which shift the resonance peaks of all four MRRs to central frequency (193.1 THz), and to adjacent and extreme frequencies of the C-band in accordance with ITU-T G.694.1 standard for the frequency grid of 12.5 GHz. These values are multiple to the minimum pitch 5 mV that the control voltage may change with.

As the calculation results show (Table 3), the sets of control voltages at MRR corresponding to the adjacent values of the working wavelength of emission, differ from each other quite strongly, so that the emission wavelength is unambiguously detected using them.

Further the compact model method was used for the developed PIC (Fig. 1) to compare the currents of photo diodes at absent control voltage at PHS with currents of photo diodes at control detection voltage applied at PHS, which shifts the MRR transmittance peaks to a certain detected wavelength (Table 4). Currents of photo diodes at absent control voltage are indicated as I_0, and currents at detection voltage — as I. The input optical power of the signal was −10 dBm (0.1 mW), and the sensitivity of photo diodes was equal to 1 A/W. Besides, the nonlinearity of photo diodes was not taken into account.

Reduction in the currents of photo diodes observed when control detection voltage is applied to the PHS is rather significant compared to the random fluctuations.

Besides, the sensitivity of the developed PIC was also detected to the optical power. It was detected as the input optical power, at which the least value of the photo diode current is 0.5 μA, i. e. exceeds the dark current 5 times. Sensitivity of the developed PIC was −18 dBm (15.8 μW).

Therefore, PIC was developed for measurement of the emission wavelength in the C-band. The developed PIC provides for the resolution of measurement of 0.3 GHz (2.4 pm), precision of ±1 GHz (±8 pm) and sensitivity to optical power −18 dBm. The developed PIC exceeds some known analogs by resolution of measurement, and by precision of measurement is not inferior to them. PIC is developed for manufacture using, technology compatible with SOI CMOS technology, which creates the possibility of large-scale manufacture at potentially low cost of one device. This PIC may be used within the stabilization system of the emission wavelength of the C-band tunable laser in implementation of DWDM technology.

Funding

This study was supported financially by the Ministry of Science and Higher Education of the Russian Federation within the 2024-0004 FEWM project.

Conflict of interest

The authors declare that they have no conflict of interest.

References

[1] Z. Chen, X. Dong, J. Gao, Z. Yu, K. Xu, IEEE Photon. J., **17** (2), 1 (2025). DOI: 10.1109/JPHOT.2025.3555482
[2] Y. Sun, *DWDM source with precise channel spacing and good reliability*, PhD thesis (College of Science and Engineering, Minneapolis, 2025).
[3] R. Yu, R. Proietti, J. Kurumida, A. Karalar, B. Guan, S.J.B. Yoo, IEEE Photon. Technol. Lett., **24** (1), 70 (2012). DOI: 10.1109/LPT.2011.2172684
[4] M. Muneeb, A. Ruocco, A. Malik, S. Pathak, E. Ryckeboer, D. Sanchez, L. Cerutti, J.B. Rodriguez, E. Tournie, W. Bogaerts, M.K. Smit, G. Roelkens, Opt. Express, **22** (22), 27300 (2014). DOI: 10.1364/OE.22.027300
[5] S.S. Kosolobov, I.A. Pshenichnyuk, K.R. Taziev, A.K. Zemtsova, D.S. Zemtsov, A.S. Smirnov, D.M. Zhigunov, V.P. Drachev, Phys. Usp., **67** (11), 1153 (2024). DOI: 10.3367/UFNe.2024.09.039762
[6] W. Bogaerts, L. Chrostowski, Laser Photon. Rev., **12** (4), 1700237 (2018). DOI: 10.1002/lpor.201700237
[7] A. Volpini, D. Massella, D. Alvarez-Outerelo, F. Soares, F.J. Diaz-Otero, in *2023 IEEE Photonics Society Summer Topicals Meeting Series (SUM)* (IEEE, 2023), p. 1–2. DOI: 10.1109/SUM57928.2023.10224439

Table 4. Estimated values of photo diode currents at absent control voltage and applied control detection voltage

f, GHz	PD1		PD2		PD3		PD4	
	I_0, μA	I, μA	I_0, μA	I, μA	I_0, μA	I, μA	I_0, μA	I, μA
195.90	20.23	4.46	23	5	23.08	4.31	20.22	3.22
193.1125	20.09	4.44	23.75	5.3	22.31	4.44	20.14	3.17
193.1	19.21	4.46	23.67	5.15	23.67	4.5	20.16	6.33
193.0875	19.56	4.44	22.52	5.15	23.75	4.44	20.17	3.18
191.60	11.18	4.43	21.5	5.18	23.88	4.44	20.05	3.21

[8] Q. Liu, Y. Bian, J. Xiong, Photonics, **12** (9), 928 (2025). DOI: 10.3390/photonics12090928
[9] Y. Liu, U. Khan, W. Bogaerts, Opt. Express, **33** (6), 13530 (2025). DOI: 10.1364/OE.558406
[10] S. Hassan, D. Chack, Microelectron. J., **104** (4), 104887 (2020). DOI: 10.1016/j.mejo.2020.104887
[11] B. Stern, K. Kim, H. Gariah, D. Bitauld, in *Frontiers in Optics + Laser Science 2023 (FiO, LS)* (Optica Publ. Group, 2023), paper FM6D.4. DOI: 10.1364/FIO.2023.FM6D.4
[12] K. Qian, J. Tang, H. Guo, W. Liu, J. Liu, C. Xue, Y. Zheng, C. Zhang, Sensors, **17** (1), 100 (2017). DOI: 10.3390/s17010100
[13] M. Hasan, G.M. Hasan, H. Ghorbani, M. Rad, P. Liu, E. Bernier, T. Hall, Opt. Express, **32** (6), 8697 (2024). DOI: 10.1364/OE.509659

Translated by M.Verenikina